Aerosol Science and Technology

ISSN: 0278-6826 (Print) 1521-7388 (Online) Journal homepage: https://www.tandfonline.com/loi/uast20

A Unique Online Method to Infer Water-Insoluble Particle Contributions

Daniel Short, Michael Giordano, Yifang Zhu, Phillip M. Fine, Andrea Polidori & Akua Asa-Awuku

To cite this article: Daniel Short, Michael Giordano, Yifang Zhu, Phillip M. Fine, Andrea Polidori & Akua Asa-Awuku (2014) A Unique Online Method to Infer Water-Insoluble Particle Contributions, Aerosol Science and Technology, 48:7, 706-714, DOI: 10.1080/02786826.2014.916778

To link to this article: https://doi.org/10.1080/02786826.2014.916778

Aerosol Science and Technology, 48:706–714, 2014

ISSN: 0278-6826 print / 1521-7388 online
DOI: 10.1080/02786826.2014.916778

A Unique Online Method to Infer Water-Insoluble Particle Contributions

Daniel Short,[1,2] Michael Giordano,[1,2] Yifang Zhu,[3] Phillip M. Fine,[4] Andrea Polidori,[4] and Akua Asa-Awuku[1,4]

[1]*Department of Chemical and Environmental Engineering, University of California—Riverside, Riverside, California, USA*
[2]*College of Engineering, Center for Environmental Research and Technology, University of California—Riverside, Riverside, California, USA*
[3]*Department of Environmental Health Sciences, University of California—Los Angeles, Los Angeles, California, USA*
[4]*South Coast Air Quality Management District, Diamond Bar, California, USA*

Particle number, size, and composition information is important for constraining aerosol effects on air quality, climate, and health. The composition of particles, especially from vehicular sources, may contain insoluble black carbon (BC) materials that modify particle nucleating properties. In this study, we develop a method to provide quantitative and real-time information on the water-insoluble components found in near-road aerosol sources. A water-based condensation particle counter (W-CPC) and a butanol-based CPC (B-CPC) were used to measure the particle number concentration. Both instruments were coupled with a scanning mobility particle sizer (SMPS) to record the particle number and size data. Real time water-insoluble particle mass was estimated from the difference in particle number concentration between the two CPCs; theoretical water-insoluble mass was calculated from the ideal hygroscopicity single parameter κ-values. This online method was calibrated with test compounds and then applied to data collected from a field study. Ambient aerosol was sampled from a monitoring station located 15 m from the I-710 freeway in Long Beach, California. The results show that near-roadway emissions contain water-insoluble (BC and non-BC) components. Particle number and BC concentrations increase after changes in wind direction near the freeway on both weekday and weekend measurements. Particles were less hygroscopic ($\kappa \sim 0.2$) before changes in wind direction from downwind to upwind of the freeway ($\kappa > 0.6$). Rapid changes in water-solubility can be captured with this technique. By assuming a two-component mixture, the water-insoluble mass fractions were inferred. BC shows a positive correlation with the water-insoluble mass however its presence may not account for the entire water-insoluble mass from the near-roadway source.

Received 23 August 2013; accepted 13 April 2014.
Address correspondence to Akua Asa-Awuku, Department of Chemical and Environmental Engineering, University of California—Riverside, 900 University Avenue, Riverside, CA 92507, USA. E-mail: akua@engr.ucr.edu
Color versions of one or more of the figures in the article can be found online at www.tandfonline.com/uast.

1. INTRODUCTION

The mass, size, and water-insoluble chemical composition of particulate matter with aerodynamic diameter equal to or less than 2.5 μm ($PM_{2.5}$) significantly affects air quality, climate, and human health (Avol et al. 1979; Charleston et al. 1992; Davidson et al. 2005; Nel et al. 1998; Pope and Dockery 2006). Carbonaceous materials, such as black carbon (BC), can contribute to water-insoluble $PM_{2.5}$ and their subsequent effects on health and climate. BC is formed from the incomplete combustion of fossil fuels and biomass (Novakov et al. 2000) and can have a peak mode below 100 nm in diameter (Rose et al. 2006). BC is defined as light absorbing material formed by the incomplete combustion of fossil fuels and biomass. BC is emitted from both anthropogenic and natural sources. Thus, the BC combustion species is operationally defined by the method of detection. Here, BC is quantified by the ability of a material to absorb energy at a 670 nm wavelength. BC aerosol is often considered water-insoluble when freshly emitted but can add water-soluble materials in surface oxidation and condensation reactions during its atmospheric lifetime (Cooke and Wilson 1996; Koehler et al. 2009; Snider et al. 2010; McMeeking et al. 2011). Hence, as a BC particle ages, the particle can modify its overall water-insoluble fraction, hygroscopic properties, and reduce the critical water-vapor saturation required to initiate heterogeneous nucleation (Zhang et al. 2008). BC has garnered recent attention due to its complex and transient role in the atmosphere (e.g., but not limited to Ramanathan and Carmichael 2008; Liggio et al. 2012; McMeeking et al. 2011). Freshly emitted BC can absorb radiation and heat the surrounding air (Conant et al. 2002;

Chung and Seinfeld 2005; Forster and Ramanswamy 2007). However, as additional water-soluble (or nonrefractory materials) condense on the surface, the particle can directly reflect sunlight and have a cooling effect that can reduce temperatures at the earth's surface (Bond et al. 2004). The real-time contribution of BC to the water-insoluble mass is important for our intrinsic understanding of ambient particles and must be quantified. In this study, we present and test a unique method to estimate BC contributions to the inferred water-insoluble mass from real-time particle counts.

Real-time particle concentrations can be measured using a condensation particle counter (CPC). One of the earliest particle concentration counters was introduced by Aitken et al. (1890–1891) and counted condensed particles with a magnifying glass. The first CPC that used Kelvin-effect measurement principles to size particles was developed in 1935 (Junge 1935) and is now the most-widely used method. In the 1970s, the saturation tube, growth tube, and optical particle techniques were implemented to improve aerosol counting measurements (Rosen et al. 1974; Bricard et al. 1976). One of the first commercial CPCs was developed in 1980 by TSI, Inc. (Agarwal and Sem 1980) and uses the same measurement principles as the CPCs used in this study.

The lower limit of particle detection for CPCs is defined by the 50% particle activation efficiency or ε_{50}. The ε_{50} of a CPC is calculated by plotting the ratio of particles counted by two distinct counting devices at varying diameters. For commercial CPC calibration, counts are compared with data from an aerosol electrometer (an instrument that counts particles based on net charge). Above the ε_{50} diameter, larger particles will likely activate, form droplets, and be detected. Hence, there are fewer statistical counting errors above ε_{50}.

Modern butanol-based CPCs (B-CPC) can detect aerosols with a lower size limit of 3 nm (Stolzenburg and McMurry 1991). Yet stored butanol is flammable and the exhaust from the CPC can be toxic if not properly vented. To address these safety concerns, a commercial continuous-flow water-based CPC (W-CPC) was introduced to the market in 2003 (Hering et al. 2005). The reported ε_{50} for ambient particles away from major roadway particle sources is 4.7 nm for the TSI 3785 W-CPC (Liu et al. 2006). A newer version of the W-CPC (TSI Model 3786) has $\varepsilon_{50} = 2.4$ nm for ambient particles. Hermann et al. 2007 reported a $\varepsilon_{50} = 7.6$ nm for the TSI 3785 Model W-CPC and $\varepsilon_{50} = 7.8$ nm for the TSI Model 3772 B-CPC for silver particles. The reported W-CPC ε_{50} diameter was comparable to the B-CPC counting efficiency for silver particles. However, adjustments in the temperature gradients between the saturation and growth tubes within the CPC can alter the ε_{50} diameter. An increased difference in temperature between the saturation and growth tubes in the W-CPC can also decrease ε_{50} diameters (Petäjä et al. 2006). Petäjä et al. (2006) reports that the ε_{50} of silver particles ranged from 4 to 14 nm with a temperature difference of 55°C to 15°C, respectively.

There are few studies that directly compare the differences between the B-CPC and W-CPCs. Previous studies discuss the discrepancies that exist. Franklin et al. (2010) showed a correlation between 1% of measured geometric mean diameter of the W-CPC TSI Model 3786 and the B-CPC TSI Model 3025 for low sulfur diesel particle diameters above 10 nm. Biswas et al. (2005) and Herring et al. (2005) have shown sensitivity toward particle counting abilities of the W-CPC for particles that range below 30 nm for ambient particle measurements. Mordas et al. (2008) concluded that the efficiency of the W-CPC (TSI 3786) was dependent on the chemical composition of the particle but provided little or no chemical information. Kulmala et al. (2007) presented a method that used four CPCs consisting of an ultrafine W-CPC, ultrafine B-CPC, W-CPC, and B-CPC called a condensation particle counter battery (CPCB). The CPCB is used to infer chemical composition information of newly formed particles between diameters of 2 to 20 nm. Kulmala et al. (2007) CPCB study aligns the ε_{50} diameter ($\varepsilon_{50} = 11$ nm) for both the W-CPC and B-CPC. In CPCB operation, a hygroscopic particle lowers the ε_{50} diameter; the W-CPC will measure a larger particle concentration than the B-CPC. A study with the CPCB in the Boreal Forest finds new particle formation compositions have a strong affinity for water (Riipinen et al. 2009) and therefore the comparison of CPCs can determine the hygroscopicity of a particle up to 20 nm. A similar exploitation between the butanol and water based instruments but different method is explored in our study to understand the effects of chemical composition on the lower detection efficiency.

In this study, we quantify the particle hygroscopicity parameter with simultaneous particle detection in butanol and water-based CPCs. The developed theory, derived from classical thermodynamics of droplet formation, estimates the water-insoluble mass in particle compositions. A late model W-CPC, with smaller instrument temperature gradient, was used to exploit the theoretical differences in particle counting measurements that can be used to infer the water-insoluble mass. The method was calibrated with known simple organic and inorganic aerosol compositions, and the experimental set-up (Section 2.1) was applied to a field study. The differences in the two CPC instruments provide quantitative and real-time information on the water-insoluble component found in near-road aerosol sources.

2. THEORY AND ANALYSIS

2.1. Water-Insoluble Mass Estimates Method

The method described here uses a W-CPC and B-CPC with two separate electrostatic classifiers and differential mobility analyzers (DMAs). When operated in scanning mode to rapidly size and count electrical mobility particle distributions, the unit is often referred to as a scanning mobility particle sizer (SMPS). Two SMPS units were used

for this analysis; one with a B-CPC and the other with a W-CPC. Each unit consists of a TSI 3080 Electrostatic Classifier with a TSI 3081 DMA and CPC. The experimental setup is shown in Figure S1 (see the online supplementary information). The SMPS samples a polydispersed flow of particles and charges particles with a Krypton-85 radioactive source. An equilibrium charge distribution was applied to particles entering the DMA. Then, the electrical mobility of the particles size selects particles into a monodisperse flow (Wang and Flagan 1990). The dry monodispersed particles then flow into the CPC; the concentration of size-selected particles was measured. The SMPS was connected to either a B-CPC (TSI Model 3772) or a W-CPC (TSI Model 3785). Both CPCs were synchronized and verified to be scanning on the same universal time. Because CPCs were not connected to the same electrostatic classifier during the field study, the ε_{50} values were averaged over a 10 min period. This ensured both CPCs were counting the same particles during the averaging period. Each electrostatic classifier has a scan time of 2.25 min with a sheath flow rate of 10 L/min. A total of four scans were performed for each 10 min average; four ε_{50} were calculated for each averaged value. We report differences in CPC particle counts below 250 nm by taking the ratio of particle concentrations from the water and butanol based counting instruments. For our analysis, it was assumed that the B-CPC counts all particles measured in the DMA selected size range. The differences in CPC particle counts were used to estimate the water-insoluble mass (Section 2.3). Discrepancies between the W-CPC and B-CPC, especially those between the minimal detectable size (10 nm and 40 nm) were attributed to particle solute properties. Unlike the CPCB, our method size selects each particle. In addition, the CPCs were not calibrated to have the same ε_{50}. Thus, the method presented here can determine the particle hygroscopicity parameters for much larger particle diameters (up to 40 nm, given the TSI 3785 set-point water-vapor saturation). The 40 nm limit is estimated from the thermodynamic models discussed in the next section.

2.2. Droplet Growth in CPCs

In CPCs, dry particles are exposed to a high relative humidity, or saturated vapor of the working fluid. Saturation, S, is the ratio of partial pressure (P_v) to the saturation vapor pressure (P_{sat}) of the working fluid. After the particles exposure to saturated conditions, the B-CPC employs a cooled growth tube to condense the working fluid vapor on the particle surface, which initiates wet droplet growth. For butanol-based instruments, it is assumed that activation depends on the Kelvin effect and the maximum S encountered along the particle trajectory through the condenser (Stoltzenberg and McMurry 1991).

The process to form wet particles in the W-CPC is different. The initial saturation area in the W-CPC is cool; the W-CPC uses a cold growth tube to produce the saturated working fluid vapor followed by a wetted/warm-walled condenser to grow wet particles (Hering et al. 2005). When the particle passes through the condenser, the mass transfer of water vapor is faster than the thermal transfer of heat to the aerosol flow. Lower molecular weight water vapor molecules diffuse more quickly, from the wetted/warm wall, to the particle surface than air and water molecules condense in the saturated environment. Dry particles are wetted, activated and grow to sizes detected by the optical counter.

Here, we present the robust theory of chemical effects for droplet formation and then explain the simplifications and assumptions used from the original theory for our analysis. The heterogeneous condensation of water vapor into the particulate phase can be predicted with Köhler Theory (Köhler 1936).

$$S = \frac{P_v}{P_{\text{sat}}(T)} = a_b \ \ exp\left(\frac{4M_b\sigma_b}{\rho_b RTD}\right) \qquad [1]$$

where R is the universal gas constant, T is the temperature at activation, D is the wet droplet diameter, ρ_b is the density of the bulk fluid condensing onto the particle (water or butanol), M_b is the molecular weight of the bulk fluid, and σ_b is the surface tension at the droplet vapor/liquid interface. a_b is the activity of the bulk fluid. Köhler theory is the combination of the Kelvin effect that increases vapor pressure and the dissolved solute effect that decreases vapor pressure at the droplet surface. When solute effects are negligible, $a_b = 1$. Equation (1) reduces to the Kelvin term. Thus, a maximum critical saturation, S_c, exists for which a minimum layer of water is required to form a droplet. S_c is greater than one and critical supersaturation, s_c, $(S_c - 1)$ is commonly used in its place. For dry particles greater than 40 nm exposed to water or butanol $s_c > 2\%$, the Kelvin term dominates and the dry particle will experience uncontrollable droplet growth. Assuming the Kelvin effect is ideal and governed by the fluid properties, changes in particle activation for a given fluid are thus controlled by the dissolved solute properties and the activity of the droplet solution. The water activity, a_w, is approximated by Raoult's Law where a_w is equivalent to the mole fraction of water in droplet solution. Rearrangement of Equation (1) yields (Seinfeld and Pandis 2006);

$$\ln s_c = \left(\frac{4A^3}{27B}\right)^{1/2}, \ A = \frac{4M_b\sigma_b}{\rho_b RT} \text{ and } B = \frac{6n_s M_b}{\pi\rho_b} \qquad [2]$$

where n_s is the moles of solute and ν is the ion dissociation of the particle in water. For a spherical solute particle, n_s is related to the dry particle diameter, d_s, the density of the

particle, ρ_s and the molecular weight of the particle, M_s such that s_c and d_s are related as follows:

$$\ln s_c^2 = \frac{4A^3\rho_b M_s}{27\nu\rho_s M_b d_s} \quad [3]$$

For an instrument with s_c, d_s is equal to the theoretical ε_{50} diameter. Köhler theory requires explicit chemical information of each solute species present. For unknown and rapidly changing particle composition, the full Köhler theory is complex. The theory can be simplified to predict the activation behavior of soluble and insoluble particle mixtures.

2.3. Water-Insoluble Mass Fraction Estimates

Traditional Köhler theory can be rewritten in terms of a single solute parameter called κ-Köhler theory. a_w is parameterized as follows (Petters and Kreidenweis 2007a,b):

$$\frac{1}{a_w} = 1 + \kappa\frac{V_s}{V_w} \quad [4]$$

where V_s is the volume of the solute, V_w is the volume of water, and κ is the hygroscopicity parameter. For multicomponent system at equilibrium the Zdanovskii, Stokes, and Robinson (ZSR) assumption is applied. A simple mixing rule is derived for which

$$\kappa = \sum_i \varepsilon_i\kappa_i \quad [5]$$

where ε_i is the component volume fraction of species and κ_i is the hygroscopicity parameter of that component.

The parameter κ characterizes the effects of solute composition for droplet activation. κ-values can range from 0 to 1; where 0 is less hygroscopic but wettable and 1 is a very hygroscopic solute. The κ value is calculated from direct measurements of d_s (or ε_{50}) measurements at a fixed instrument s_c as follows:

$$\kappa = \frac{4A^3}{27d_s^3\ln^2(s_c)} \quad [6]$$

The κ-Köhler theory (Equation (6)) is similar to Equation (3) but assumes the σ_b properties of the droplet are that of the pure fluid. Changes in measured κ values suggest chemical changes in solute composition (Petters and Kreidenweis 2007a,b). The changes in composition can be approximated with a two-component model of low hygroscopic and highly hygroscopic solute material. In this study, we choose sulfuric acid (SA) and dioctyl phthalate (DOP) as a proxy two-component mixture. SA has been measured in vehicular diesel exhaust, and is believed to be a key nucleation gas component in engine new particle formation (Tobias et al. 2001; Arnold et al. 2006; Arnold et al. 2012). SA is highly hygroscopic and has a $\kappa_{sa} = 0.9$ (Petters and Kreidenweis 2007a,b). Motor vehicle particulate composition (up to 95%) is dominated by unburned lubricating oil and fuel spectral signatures (Schauer et al. 1999; Tobias et al. 2001; Sakurai et al. 2003). DOP has been previously used as a proxy for hydrophobic but wettable aerosol from vehicular exhaust (Asa-Awuku et al. 2009). DOP is a diester of phtlaic acid with $\kappa_{DOP} \approx 0.01$.

The two-component mixtures were applied for two reasons (1) the simple model must comprise of materials that may be found near major roadway sources and (2) each component must have distinct water-affinities, preferably approaching realistic limits of the single parameter, κ-hygroscopicity. By assuming a unit particle density and a two-component mixture, we infer the water-insoluble mass fraction, χ with Equation (7).

$$\kappa_{am} = \kappa_{sa}(1-\chi) + \kappa_{DOP}(\chi) \quad [7]$$

where, κ_{am} is the hygroscopicity of ambient unknown composition (Equation (6) and Section 2.3). The κ_{am} is also an indication of the hygroscopic fraction (assuming ideal Kelvin with a two component hygroscopic and a low hygroscopic core with $\kappa = 1$ and 0, respectively). Equation (7) is a modified approximation accounting for likely hygroscopic and a low hygroscopic, but wettable, components found in vehicular exhaust. Equation (7) is a form of Equation (5), where the water-insoluble volume fraction, χ, relates specifically to DOP and κ_i is the κ of either SA or DOP. κ_{am} is derived from measurements using Equation (6), where only the χ term is unknown. The SA and DOP two-component model (Equation (7)) provides conservative estimates of χ within 15% uncertainty. 15% uncertainty is derived from the variability of κ_{am} in section 3.2. The uncertainty includes 10% error in particle counting from CPC instrumentation. In follow-up work, Petters and Kreidenweis (2007b, 2013) discussed the limitations of partially soluble species and surfactant partitioning in κ-Köhler theory. As with traditional Köhler theory, chemical speciation is required to account for the nonideal solubility and surfactant tension effects in the extension of κ-Köhler theory. In this study, we utilize the single parameter first posed in Petters and Kreidenweis (2007a,b) that assumes a complete soluble and insoluble species exists to provide fast measurements of particle hygroscopicity. If the size distribution is assumed to be internally mixed (a uniform composition is applied to each size), we can estimate the mass of water-insoluble material as χ multiplied by the particle volume distribution and unit density.

2.3.1. *External Mixing State Effects*

In complex aerosol, there are multiple chemical species that can inhibit droplet activation. These chemical species may be

indicative of an external mixture of two distinct soluble populations at different sizes. These populations will produce two separate ε_{50} diameters, which will also produce multiple κ_{am}. The weighted average of multiple κ_{am} represents the varying chemical composition. The corresponding water-insoluble mass fractions, χ, can be averaged to provide an overall water-insoluble mass fraction. Each corresponding water-insoluble mass fraction is solved with Equations (6) and (7). Once an overall water-insoluble mass fraction is calculated, Equations (6) and (7) are rearranged to solve for an overall κ_{am} and overall ε_{50}.

2.4. Method Calibration and Analysis

The water-insoluble mass estimate method was calibrated with atomized ammonium sulfate, sodium chloride, and DOP. For calibration, the atomized aerosol is dried and size selected with the TSI Model 3081 DMA. The monodisperse stream was split and the W-CPC and B-CPC sample at a rate of 1 LPM, respectively. For a given particle diameter, the ratio of W-CPC counts was divided by B-CPC counts. The data selected for each scan of the size distribution is similar to a cloud condensation nuclei (CCN) activation curve; the ratio of activated water droplets to total particles versus particle diameter is plotted. This economical method is similar to the use of a CCN counter with a $s_c = 2\%$ to retrieve κ values for the measured particles. A sigmoidal equation was fit to the data to find the diameter corresponding to a ratio of 0.5. Figure S2 shows the curve for both ammonium sulfate, sodium chloride and DOP. The ratio of 0.5 is the ε_{50} that is assumed to be the minimum diameter for droplet activation and subsequently used to calculate κ. Again, κ was calculated in Equation (5) with the only unknown parameter, ε_{50}. This same method for calculating κ was also used to calculate the ambient hygroscopicity near roadway (κ_{am}), obtained from during the field study. The ε_{50} measured for calibration ammonium sulfate aerosol was 16.9 nm, as shown in Figure S2. A 16.9 nm critical diameter is used in Equation (6) to calculate the single hygroscopicity parameter, κ. κ for the calibration is 0.62 within ± 0.1 of published and theoretical values for the CCN activation of ammonium sulfate (Petters and Kreidenweis 2007a,b). The calibration procedure was repeated with DOP. For DOP $\kappa <$ 0.00804 and $\varepsilon_{50} = 71.3$ nm; consistent with wettable but low-hygroscopic material (Figure S2). In addition, the calibration procedure was repeated for sodium chloride. $\kappa = 1.38$ and $\varepsilon_{50} = 12.9$ nm for NaCl. The measured κ for sodium chloride is ± 0.1 to the literature value of 1.28 (Petters and Kreidenweis 2007a,b). Each of the calibration solution ε_{50} measurements were measured with the same instrument critical supersaturation (s_c) at 2%. It was assumed that the presence of multiple charged particles is negligible for our data. The calibration data agrees well with literature values thus supporting this assumption. The experimental analysis was applied to ambient aerosol measurement to infer real-time water-insoluble mass estimations. Thus, in addition to the field measurement, the proposed experimental method was also tested with known aerosol in controlled settings.

2.5. BC Measurement and Analysis

BC mass concentration was measured with a multiangle absorption photometer (MAAP). The MAAP is a filter-based measurement that uses one light source at 670 nm to produce photons directed toward an accumulation of particles on Teflocarbon filter paper (Petzold and Schönlinner 2004). The back scattering of these photons was then measured by four photodetectors located at 45 degree intervals. As particles accumulate on the filter paper, the light transmitted back or above the filter paper correlates to the concentration of BC. A photodetector below the filter paper determines the upper limit of detection. The upper limit occurs when <10% of light emitted is transmitted through the filter paper. Once this is achieved, clean filter paper is moved on to the detection area for continuous online BC measurements. Calibrating the instrument requires a known amount of BC that is aerosolized and then analyzed with the MAAP. Aquadag© aqueous solution is atomized and then dried. The Aquadag© BC mass concentration is simultaneously measured with an aerosol particle mass (APM, Kanomax model 3600) analyzer (Schwarz et al. 2006) and the MAAP. After calibration, The MAAP BC concentrations agree to within $\pm 11\%$ of APM measurements.

2.6. Field Study Location

The Interstate Highway 710 (I-710) is a major truck route in Southern California. Approximately 20% of the I-710 total traffic flow is comprised of heavy-duty trucks. Measurements were taken 15 m east (and mostly downwind) of the I-710, on the southbound side of the freeway near the intersection with Long Beach Blvd. on May 10th (weekday) and 14th, 2011 (weekend). There were no other significant sources of particles other than the highway traffic emissions. Data were provided for the days which simultaneous sizing and counting instrumentation is available. All instruments were housed inside one of SCAQMDs air conditioned monitoring trailers. Five minute average traffic information (i.e., total and heavy duty diesel

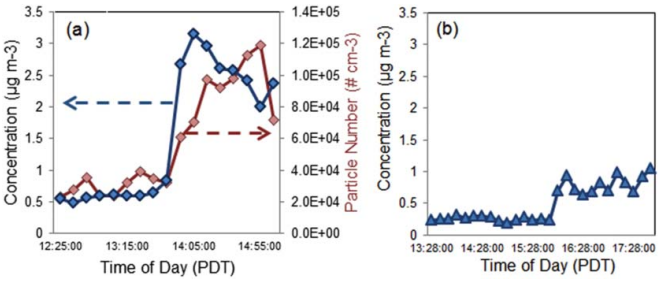

FIG. 1. Ten minute averaged black carbon (BC) and particle number (PN) concentrations from water-based (W-CPC) particle concentrations on the weekday (a) and only averaged BC concentrations on the weekend (b).

traffic flows) on the north and southbound I-710 lanes were retrieved from Caltrans website (http://pems.dot.ca.gov). Meteorological instrumentation recorded wind direction and velocity data (Figure S3).

3. RESULTS AND DISCUSSION

3.1. BC and Particle Number Concentration

Fewer than 200 trucks and ~1000 cars per 5 min traversed the I-710 highway on the weekday and weekend. The concentration of cars and trucks (Figure S4) showed small variations for both days. However, significantly less vehicles traveled on the highway during the weekend. On both days, wind and particle instrument measurements increase in magnitude/direction in the late afternoon (14:00 and 16:00 PDT, pacific daylight time). A significant change in wind direction from downwind to upwind of the freeway occurs for both the BC and total particle concentrations (Figure 1a). Downwind aerosol measurements are considered to be when freeway aerosols were flowing in the opposite direction of the sampling inlet. Whereas, upwind aerosol measurements are defined as when the freeway aerosols were flowing in the direction of the sampling port inlet. Data showing the total particle concentration measured with a W-CPC (TSI Model 3781) was only available for the weekday measurements during the campaign. The BC concentration for both days (Figure 1), reached a maximum 10 min average concentration of 3 μg m^{-3} and 1 μg m^{-3} at 14:00 and 16:00 PDT for the weekday and weekend measurements, respectively. The measurements were averaged every 10 min with a lower detection limit of 0.1 μg m^{-3}. BC concentrations on the weekend are lower compared to the weekday concentrations. Lower BC concentrations are likely due to fewer weekend heavy-duty vehicle traffic (Figure S4).

3.2. Particle Size Distribution

The particle counts of both the W-CPC and B-CPC instruments were compared to infer solute properties. Ten minute average was applied to the particles counts for each particle diameter of each instrument. Ten minute averages account for size distribution number and variability of four size distribution scans (2.25 min each) taken with the SMPS. A ratio of the W-CPC to B-CPC particle count averaged data was calculated. Again, ε_{50} is calculated from the ratio of W-CPC and B-CPC particle counts which was used to calculate κ_{am} (Equation (5)). We note that there were occurrences in our dataset, especially above the 200 nm regime, where the W-CPC recorded greater particle counts than the B-CPC. For these occurrences at high instrument s_c, particle size (surface area) is more important for droplet activation than solute composition. Thus, we focus our comparison on the discrepancies near or below 40 nm.

Figure 2 shows the relationship between two CPCs for the weekday and weekend. There were fewer particle counts in the W-CPC data compared to the B-CPC data. The instruments agree above the 30 nm particle diameter range.

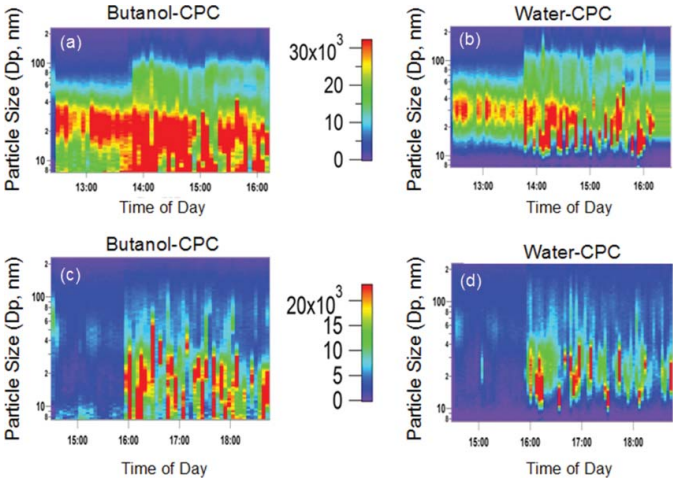

FIG. 2. The weekday particle size and number distributions measured with a (a) B-CPC and (b) W-CPC. The weekend particle size and number distributions measured with a (c) B-CPC and (d) W-CPC. The scale between the figures shows particle number concentration (# cm^{-3}).

Figures 2a and b show a large increase in particle counts after 14:00 h. The increase in particle number concentration correlated to the change in sampling wind direction (downwind to upwind, Figure 1). Lower particle number concentrations persist during the weekend. The weekday and weekend diurnal profiles are similar. Fewer particles were measured during the weekend. The B-CPC size distributions had a majority of weekend particle counts below the 40 nm range (Figure 2c). The W-CPC size distribution (Figure 2d) show fewer particles below the 30 nm range (similar to the comparison of weekday measurements Figures 2a and b). Figure 2c and d shows an increase in particle concentration at 16:00 h, which is due to the change in wind direction.

The ratio of particle number concentrations measured by B-CPC and W-CPC is shown in Figure 3. Before changes in wind direction on the weekday (Figure 3a), the W-CPC measured fewer than 50% of the particles below 30 nm measured by the B-CPC. Hence, a gradual change in the activation ratio occurs as particles increase in size (observed via the changing color gradient in Figure 3). Before the change in wind direction on the weekend (Figure 3b), the W-CPC measures 50%

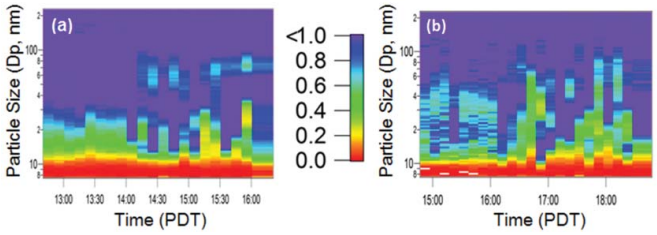

FIG. 3. The comparison of water to butanol particle concentration counts (ratio from 0 to 1) for the (a) weekday and (b) weekend measurements.

of the particles at a range of sizes below 100 nm. However, the CPC count ratio was more variable on the weekend than on the weekday (Figure 3). The diameter for which the W-CPC measures 50% or more of the total particles occurs at sizes above and below 30 nm for the upwind weekend measurements.

Figure 4 shows the aerosol ε_{50} and calculated κ_{am} values for sampling downwind and upwind of the freeway. As ε_{50} increases, κ_{am} decreases. A sample activation plot is shown in Figure S5 for the weekday and weekend, which is used to determine ε_{50}. Multiple ε_{50} values were shown from upwind of the freeway aerosol. The average ε_{50} was used to calculate κ_{am} values for multiple ε_{50} (Section 2.3.1). The weekend has more of these multiple ε_{50} which accounts for the variation in ε_{50} (Figure S5). The overall hygroscopicity parameter decreases ($\Delta\kappa_{am} \sim 0.35$) for upwind aerosols on both days. Despite changes in traffic patterns and overall particle concentrations, κ_{am} was greater than 0.6 (very hygroscopic) in the morning hours and then becomes less than 0.2 (slightly hygroscopic). Though there were significantly more particles emitted during the weekday (Figure 2), the composition of particles on the weekday and weekends were similar. The changes in particle soluble composition were dominated by changing wind direction aerosol sampling rather than traffic volume.

3.3. Inferred Water-Insoluble Mass

Figure 5 correlates the inferred water-insoluble mass and BC mass concentration. The water-insoluble mass was estimated from the particle volume distributions and κ_{am} (Figure 4). The total particle mass was estimated using the aerosol size distributions measured from the B-CPC particle number, assuming a density of 1 g/cm^3. A density of 1 g/cm^3 was used as an estimate for the density of the particles sampled since density information was not measured. Turpin and Lim (2001) determined the density of the Los Angeles Basin aerosol was about 1.2 g/cm^3. The difference in prescribed and literature roadway source aerosol density is within 25%. The weekday data points correlate to a slope of 1 to 1; whereas the weekend data points correlated to the 2 to 1 line (Figure 5). The majority of these points were within 25% of the slopes (dotted lines in Figure 5). During the weekday BC mass concentrations

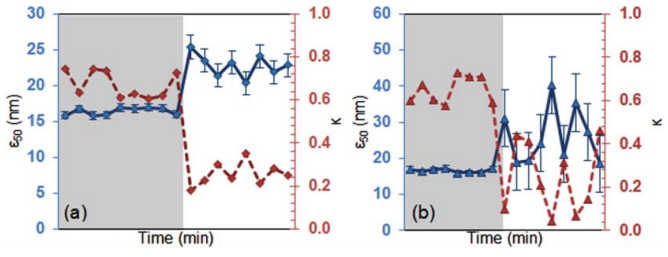

FIG. 4. Changing κ (dashed line) and ε_{50} (solid line) for both weekday and weekend data sets. The shaded region represents the time before the wind change.

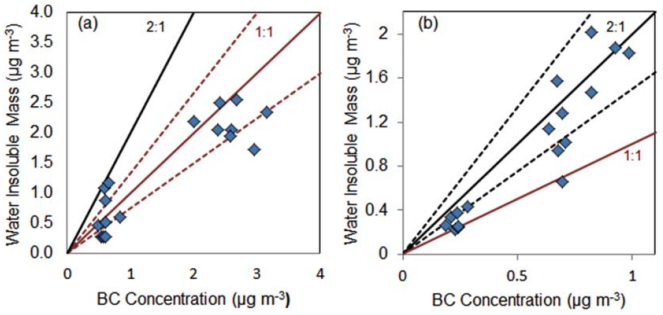

FIG. 5. Black carbon concentration versus inferred water insoluble mass from the weekday (a) and weekend (b) measurements. The solid line shows the rate of increase; either 1:1 for the weekday and 2:1 for weekend. Dashed lines represent 25% deviation from (a) 1:1 or (b) 2:1 solid lines.

are equivalent to the estimated particle water-insoluble mass (Figure 5a). This was determined from the data correlating with the 1 to 1 line. On the weekend, the BC concentration and the estimated water-insoluble mass data were within 25% of the 2 to 1 slope; suggesting the estimated water-insoluble mass increases more rapidly than the BC mass concentrations.

Both slopes in Figure 5 were positive and thus BC mass concentrations contribute to the estimated water-insoluble mass. We note that BC may not be the only water-insoluble component from roadway emissions. The weekend data shows a larger amount of the estimated water-insoluble mass compared to the BC mass concentration (data points correlate with the 2 to 1 line) indicating that BC is not the only water-insoluble composition. There may be other particulate compositions (i.e., lubrication oil) that can contribute to the water-insoluble mass estimates that may not absorb light at a 670 nm wavelength. Conversely, our data shows that the weekday measurements of BC material may be entirely water-insoluble; the contribution of BC was the main source of water-insoluble mass for the weekday. The unknown water-insoluble compositions contribute less than 25% uncertainty to the correlation of the water-insoluble mass estimates and BC mass concentrations for the weekday. Additionally, changes in unit particle density could contribute to the 25% deviations. Nonetheless, the data shows that the presence of BC (and other water-insoluble materials) affect counting efficiencies of the W-CPC.

4. SUMMARY

The aerosol solute composition affects the counting efficiency of W-CPC and B-CPCs. Published work confirms discrepancies exist between the two CPC instruments and can be used to infer water-affinities (Kulmala et al. 2007; Riipinen et al. 2009). In this study, two SMPS systems measured differences in particle size and number distributions with two CPCs of different working fluids. The method was used to capture quick changes in solute hygroscopicity and gain quantitative insight into the ephemeral nature of near road-way sources. Initial calibration measurements confirm that the discrepancies

in CPC readings can be attributed to the estimated water-insoluble mass and are consistent with classical thermodynamic theory. The method presented here is different than those already published, and is able to determine particle hygroscopicity up to a 40 nm particle diameter (instead of 10 nm with the method described in Kulmala et al. [2007]). The method can find critical activation diameters that are translated into a single hygroscopicity parameter, κ. The assumption that particles are a two-component mixture of highly hygroscopic and low hygroscopic compositions works well for internally mixed aerosols. In our near roadway field study, the sampled air mass particle number, composition, and estimated water-insoluble mass varied with traffic patterns and wind direction. Sampling downwind to upwind of the freeway aerosol had the greatest influence on measurements; particles from the freeway that were directly adverted to the sampling port inlet during peak traffic hours were less hygroscopic than those measured earlier in the day. The fresh vehicular emissions contained higher concentrations of BC and water-insoluble material that were less likely to nucleate in the W-CPC. The particle number concentrations that contained water-insoluble material affected the counting efficiency of the instrumentation. On the weekend, the increase in the water-insoluble mass estimates was about two times the contribution of the BC. This suggests that other species (e.g., aerosol that do not absorb at 670 nm wavelengths) were present and water-insoluble. Thus, other water-insoluble species from near-roadway sources may affect the efficiency of water-based condensational particle counting instrumentation. Additional chemical composition measurements (not available during this field study) can provide further insight into the total particle composition. The coupling of CPCs with different working fluids can provide fast and real-time evidence of changes in hygroscopic composition. A conservative estimate of the water-insoluble mass fraction from traffic-related aerosols can be inferred using a two-component mixture of wettable hydrophobic material and highly hygroscopic solute.

ACKNOWLEDGMENTS

The authors would also like to thank Dr. Wayne Miller for his support in facilitating collaborations on the project. The South Coast Air Quality Management District (SCAQMD) is also acknowledged for their support in the use of facilities and additional expertise for the study.

FUNDING

The authors would like to thank the U.S. Environmental Protection Agency for funding this work, made possible by EPA grant number 83504001. Its contents are solely the responsibility of the grantee and do not necessarily represent the official views of the EPA. Further, the EPA does not endorse the purchase of any commercial products or services mentioned in the publication.

SUPPLEMENTAL MATERIAL

Supplemental data for this article can be accessed on the publisher's website.

REFERENCES

Agarwal, J. K., and Sem, G. J. (1980). Continuous Flow, Single-Particle-Counting Condensation Nucleus Counter. *Journal of Aerosol Science*, 11:343–357.

Aitken, J. (1890–1891). On a Simple Pocket Dust-Counter. *Proc. R. Soc. Edinb.*, 18:39–53.

Arnold, F., Pirjola, L., Aufmhoff, H., Schuck, T., Lähde, T., and Heikkilä J. (2006). First Gaseous Sulfuric Acid Measurements in Automobile Exhaust: Implications for Volatile Nanoparticle Formation. *Atmos. Environ.*, 40:7097–7105.

Arnold, F., Pirjola, L., Rönkkö, T., Reichl, U., Schlager, H., Lähde, T., Heikkilä, J., and Keskinen, J. (2012). First Online Measurements of Sulfuric Acid Gas in Modern Heavy-Duty Diesel Engine Exhaust: Implications for Nanoparticle Formation. *Environ. Sci. Technol.*, 46:11227–11234.

Asa-Awuku, A., Miracolo, M. A., Kroll, J. H., Robinson, A. L., and Donahue, N. M. (2009). Mixing and Phase Partitioning of Primary and Secondary Organic Aerosols. *Geophys. Res. Lett.*, 15:L15827

Akhter, M. S., Chughtai, A. R., and Smith, D. M. (1985). The Structure of Hexane Soot I. Spectroscopic Studies. *Appl. Spectrosc*. 39(1):143–153.

Avol, E. L., Jones, M. P., Bailey, R. M., Chang, N. M. N., Kleinman, M. T., Linn, W. S., Bell, K. A., and Hackney, J. D. (1979). Controlled Exposures of Human Volunteers to Sulfate Aerosols – Health-Effects and Aerosol Characterization. *Am. Rev. Respir. Dis.*, 120:319–327.

Biswas, S., Fine, P. M., Geller, M. D., Hering, S. V., and Sioutas, C. (2005). Performance Evaluation of a Recently Developed Water-Based Condensation Particle Counter. *Aerosol Sci. Technol.*, 39:419–427.

Bond, T. C., Streets, D. G., Yarber, K. F., Nelson, S. M., Woo, J., and Klimont, Z. (2004). A Technology-Based Global Inventory of Black and Organic Carbon Emissions from Combustion. *J. Geophys. Res.*, 109:D14203.

Bricard, J., Delattre, P., Madelaine, G., and Pourprix, M. (1976). Detection of Ultra-Fine Particles by Means of a Continuous Flux Condensation Nuclei Counter. in *Fine Particles: Aerosol Generation, Measurement, Sampling, and Analysis*, B. Y. H. Liu, ed., Academic Press, NewYork, pp. 565–580.

Charlson, R. J., Schwartz, S. E., Hales, J. M., Cess, R. D., Coakley, J. A., Hansen, J. E., and Hofmann, D. J. (1992). Climate Forcing by Anthropogenic Aerosol. *Science*, 255:423–430.

Chung, S. H., and Seinfeld, J. H. (2005). Climate Response of Direct Radiative Forcing of Anthropogenic Black Carbon. *J. Geophys. Res.*, 110:D11102.

Conant, W. C., Nenes, A., and Seinfeld, J. H. (2002). Black Carbon Radiative Heating Effects on Cloud Microphysics and Implications for the Aerosol Indirect Effect 1. Extended Köhler Theory. *J. Geophys. Res.*, 107:4604.

Cooke, W. F., and Wilson, J. N. (1996). A Global Black Carbon Aerosol Model. *J. Geophys. Res.*, 101:19395–19409.

Davidson, C. I., Phalen, R. F., and Solomon, S. (2005). Airborne Particulate Matter and Human Health: A Review. *Aerosol Sci. Technol.*, 39:737–749.

Forster, P., and Ramanswamy, V. (2007). *Climate Change 2007: The Physical Science Basis — Contribution of Working Group I to the Fourth Assessment Report of the Intergovernmental Panel on Climate Change*. Cambridge Univ. Press, Cambridge UK, New York, USA.

Franklin, L. M., Bika, A. S., Watts, W. F., and Kittelson, D. B. (2010). Comparison of Water and Butanol Based CPCs for Examining Diesel Combustion Aerosols. *Aerosol Sci. Technol.*, 44:629–638.

Hering, S. V., and Stolzenburg, M. R. (2005). A Method for Particle Size Amplification by Water Condensation in a Laminar, Thermally Diffusive Flow. *Aerosol Sci. Technol.*, 39:428–436.

Hering, S. V., Stolzenburg, M. R., Quant, F. R., O'Berreit, D. R., and Keady, P. B. (2005). A Laminar-Flow, Water-Based Condensation Particle Counter (WCPC). *Aerosol Sci. Technol.*, 39:659–672.

Hermann, M., Wehner, B., Bischof, O., Han, H., Krinke, T., Liu, W., Zerrath, A., and Wiedensohler, A. (2007). Particle Counting Efficiencies of new TSI Condensation Particle Counters. *J. Aerosol Sci.*, 38:674–682.

Junge, C. (1935). Neuere Untersuchungen an der Grossen Atmosph¨arischen Kondensationskerne. *Meteorol. Z.*, 52:467–470.

Köhler, H. (1936). The Nucleus in and the Growth of Hygroscopic Droplets. *Trans. Faraday Soc.*, 32:1152–1161.

Koehler, K. A., DeMott, P. J., Kreidenweis, S. M., Popovicheva, O., Petters, M. D., Carrico, C. M., Kireeva, E., Khokhlova, T., and Shonija, N. (2009). Cloud Condensation Nuclei and Ice Nucleation Activity of Hydrophobic and Hydrophilic Soot Particles. *Atmos. Chem. Phys.*, 11:7906–7920.

Kulmala, M., Mordas, G., Petäjä, T., Grönholm, T., Aalto, P. P., Vehkamäki, H., Hienola, A., Herrmann, E., SipiläM., Riipinen, I., Manninen, H., Hämeri, K., Stratmann, F., Bilde, M., Winkler, P. M., Birmili, W., and Wagner, P. E. (2007). The Condensation Particle Counter Battery (CPCB): A New Tool to Investigate the Activation Properties of Nanoparticles. *J. Aerosol Sci.*, 38:289–304

Liggio, J., Gordon, M., Smallwood, G., Li, S., Stroud, C., Staebler, R., Lu, G., Lee, P., Taylor, B., and Brook, J. R. (2012). Are Emissions of Black Carbon from Gasoline Vehicles Underestimated? Insights from Near and On-Road Measurements. *Environ. Sci. Technol.*, 46:4819–4828.

Liu, W., Kaufman, S., Osmondson, B., and Sem, G. (2006). Water-Based Condensation Particle Counters for Environmental Monitoring of Ultrafine Particles. *J. Air Waste Manage.*, 56:444–445.

McMeeking, G. R., Good, N., Petters, M. D., McFiggans, G., and Coe, H. (2011). Influences on the Fraction of Hydrophobic and Hydrophilic Black Carbon in the Atmosphere. *Atmos. Chem. Phys.*, 11:5099–5112.

Moosmuller, H., Chakrabarty, R. K., and Arnott, W. P. (2009). Aerosol Light Absorption and its Measurement: A Review. *J. Quant. Spectros. Radiat. Transfer*, 110:844–878.

Mordas, G., Manninen, H. E., Petäjä, T., Aalto, P. P., Hämeri, K., and Kulmala, M. (2008). On Operation of the Ultra-Fine Water-Based CPC TSI 3786 and Comparison with Other TSI Models (TSI 3776, TSI 3772, TSI 3025, TSI 3010, TSI 3007). *Aerosol Sci. Technol.*, 42:152–158.

Nel, A. E., Diaz-Sanchez, D., Ng, D., Hiura, T., and Saxon, A. (1998). Enhancement of Allergic Inflammation by the Interaction between Diesel Exhaust Particles and the Immune System. *J. Allergy Clin. Immunol.*, 102:539–554.

Novakov, T., Andreae, M. O., Gabriel, R., Kirchstetter, T. W., Mayol-Bracero, O. L., and Ramanathan, V. (2000). Origin of Carbonaceous Aerosols over the Tropical Indian Ocean: Biomass Burning or Fossil Fuels? *Geophys. Res. Lett.*, 27:4061–4064.

Petäjä, T., Mordas, G., Manninen, H., Aalto, P., Hameri, K., and Kulmala, M. (2006). Detection Efficiency of a Water Based TSI Condensation Particle Counter 3785. *Aerosol Sci. Technol.*, 40:1090–1097.

Petters, M. D., and Kreidenweis, S. M. (2007a). A Single Parameter Representation of Hygroscopic Growth and Cloud Condensation Nucleus Activity. *Atmos. Chem. Phys.*, 7:1961–1971.

Petters, M. D., and Kreidenweis, S. M. (2007b). A Single Parameter Representation of Hygroscopic Growth and Cloud Condensation Nucleus Activity-Part 2: Including Solubility. *Atmos. Chem. Phys.*, 8:6273–6279.

Petters, M. D., and Kreidenweis, S. M. (2013). A Single Parameter Representation of Hygroscopic Growth and Cloud Condensation Nucleus Activity - Part 3: Including Surfactant Partitioning. *Atmos. Chem. Phys.*, 13(2): 1081–1091.

Petzold, A., and Schönlinner, M. (2004). The Multi-Angle Absorption Photometer – A New Method for the Measurement of Aerosol Light Absorption and Atmospheric Black Carbon. *J. Aerosol Sci.*, 35:421–441.

Pope, C. A., and Dockery, D. W. (2006). Health Effects of Fine Particulate Air Pollution: Lines that Connect. *J. Air Waste Manage.*, 56:709–742.

Ramanathan, V., and Carmichael, G. (2008) Global and Regional Climate Changes due to Black Carbon. *Nature Geosci.*, 1:221–227.

Riipinen, I., Manninen, H. E., Yli-Juuti, T., Sipilä, M., Ehn, M., Junninen, H., Petäjä, T., and Kulmala, M. (2009). Applying the Condensation Particle Counter Battery (CPCB) to Study the Water-Affinity of Freshly-Formed 2–9 nm Particle in Boreal Forest. *Atmos. Chem. Phys.*, 9:3317–3330

Rose, D., Wehner, B., Ketzel, M., Engler, C., Voigtl¨ander, J., Tuch, T., and Wiedensohler, A. (2006). Atmospheric Number Size Distributions of Soot Particles and Estimation of Emission Factors. *Atmos. Chem. Phys.*, 6:1021–1031.

Rosen, J. M., Pinnick, R. G., and Hall, R. (1974). *Recent Measurements of Condensation Nuclei in the Stratosphere, Proceedings 3rd Conference Climatic Impact Assessment Program DOT-TCSOST-74-15*. Department of Transportation, Washington, D.C.

Sakurai, H., Tobias, H. J., Park, K., Zarling, D., Docherty, D. B., Kittelson, S., McMurry, P. H., and Ziemann, P. J. (2003). On-Line Measurements of Diesel Nanoparticle Composition and Volatility. *Atmos. Environ.*, 37:1199–1210.

Schauer, J. J., Kleeman, M. J., Cass, G. R., and Simoneit, B. E. T. (1999). Measurement of Emissions from Air Pollution Sources. 2. C1 through C30 Organic Compounds from Medium Diesel Trucks. *Environ. Sci. Technol.*, 33(10):1578–1587.

Schwarz, J. P., Gao, R. S., Fahey, D. W., Thomson, D. S., Watts, L. A., Wilson, J. C., Reeves, J. M., Darbeheshti, M., Baumgardner, D. G., Kok, G. L., Chung, S. H., Schulz, M.; Hendricks, J., Lauer, A., Kärcher, B., Slowik, J. G., Rosenlof, K. H., Thompson, T. L., Langford, A. O., Loewenstein, M., and Aikin, K. C. (2006). Single-Particle Measurements of Midlatitude Black Carbon and Light-Scattering Aerosols from the Boundary Layer to the Lower Stratosphere. *J. Geophys. Res.*, 111:D16207.

Seinfeld J. H., and Pandis, S. N. (2006). *Atmospheric Chemistry and Physics: From Air Pollution to Climate Change*, John Wiley & Sons, Inc., Hoboken, New Jersey.

Snider J. R., Wex, H., Rose, D., Kristensson, A., Stratmann, F., Hennig, T., Henning, S., Kiselev, A., Bilde, M., Burkhart, M., Dusek, U., Frank, G. P., Kiendler-Scharr, A., Mentel, T. F., Petters, M. D., and Põschl, U. 2010. Intercomparison of Cloud Condensation Nuclei and Hygroscopic Fraction Measurements: Coated Soot Particle Investigated During the LACIS Experiment in November(LExNo). *J. Geophys. Res.*, 115: D11205.

Stolzenburg, M. R., and McMurry, P. H. (1991). An Ultrafine Aerosol Condensation Nucleus Counter. *Aerosol Sci. Technol.*, 14:48–65.

Tobias, H. J., Beving, D. E., Ziemann, P. J., Sakurai, H., Zuk, M., McMurry, P. H., Zarling, D., Waytulonis, R., and Kittelson, D. B. (2001). Chemical Analysis of Diesel Engine Nanoparticles using a Nano-DMA/thermal Desorption Particle Beam Mass Spectrometer. *Environ. Sci. Technol.*, 35: 2233–2243.

Turpin, B. J., and Lim, H. J. (2001). Species Contributions to PM2.5 Mass Concentrations: Revisiting Common Assumptions for Estimating Organic Mass. *Aerosol Sci. Technol.*, 35:602–610

Venkatachari, P., Zhou, L., Hopke, P. K., Schwab, J. J., Demerjian, K. L., Weimer, S., Hogrefe, O., Felton, D., and Rattigan, O. (2006). An Intercomparison of Measurement Methods for Carbonaceous Aerosol in the Ambient Air in New York City. *Aerosol Sci. Technol.*, 40:788–795.

Wang, S. C., and Flagan, R. C. (1990). Scanning Electrical Mobility Spectrometer. *Aerosol Sci. Technol.*, 13:230–240.

Zhang, R. Y., Khalizov, A. F., Pagels, J., Zhang, D., Xue, H., and McMurry, P. H. (2008). Variability in Morphology, Hygroscopicity, and Optical Properties of Soot Aerosols During Atmospheric Processing. *Proc. Nat. Acad. Sci.*, 105:10291–10296.